Agronomy Research **17**(2), 447–455, 2019
https://doi.org/10.15159/AR.19.102

Assessment of production zones modelling accuracy based on satellite imaging and yield measurement of selected agriculture plot

Z. Jelínek*, K. Starý and J. Kumhálová

Czech University of Life Sciences Prague, Faculty of Engineering, Department of Machinery Utilization, Kamýcká 129, CZ165 00 Prague, Czech Republic
*Correspondence: jelinekzdenek@tf.czu.cz

Abstract. Currently, remote sensing or yield monitor equipment offer possibilities how to estimate productivity of the agriculture field. That is why the main aim of this study is to assess how the latest satellite images from vegetation season and final yield data from combine harvester can be used to predict yield and to assess site-specific zones productivity. The study is focused on the accuracy of these systems for the field productivity estimation. The 24.7 ha experimental field is located near to Vendoli village (the Czech Republic) and it is cultivated by conventional agricultural practices with emphasis on typical agricultural crops growing in the Czech Republic (winter wheat, spring barley and winter rape). The results showed that both methods of estimation can be used for yield prediction. Nevertheless, each of them need specific processing and has typical limitations.

Key words: Spectral indices, yield data, growth stages, geoinformatics.

INTRODUCTION

Agricultural systems are modified ecosystems. Change in one component of a system makes changes in other systems, because of mutual interactions. For example change in humid or in weather to warm can lead to the development of a crop diseases and losing of crop yield potential. Adaptation to managing technological processes is very difficult. Systems are influenced by the weather condition and other inputs. Murthy (2012) described nine types of agricultural meteorology models, which are classified into different types or groups, i.e statistical, mechanistic, deterministic, stochastic, dynamic, static, simulation, descriptive and explanatory model. These models explain influence of weather on agricultural systems.

Remote sensing in agricultural application has been used more than three decades (Knipling, 1970; Tucker et al., 1981; Moran et al., 1994; Wardlow & Egbert, 2008) and one of the aim of remote sensing is to optimize crop yield in large plot and predict yield (Mulla, 2013). Generally mapping of yields and weather models are important for projecting impact of climate change on linked environmental outcomes (Rosenzweig et. Al., 2013). Currently many information about individual zones are accumulated and are used for the analysis of crop growth a yield patterns and also can be used for management zones (Mulla, 2013). In studies focused on monitoring of health crop with the help of remote sensing are used especially spectral indices, mainly Normalized Difference Vegetation Index (NDVI, Rouse et al., 1974), the normalized ratio between RED and NIR bands. Most of spectral indices are based on leaf area index (LAI) or absorption photosynthetically radiation (Asrar et al., 1984; Baret & Guyot, 1991). More than 100 spectral indices have been reviewed by Xue & Su (2017). They described spectral indices along with their representativeness, applicability and implementation in precision agriculture.

Weather data is usually used as an input to crop models. Thornton et al. (1997) described these models and their link to simulation of crop growth, development and impacts of climate change. Crop models and simulation are very often used in USA and also in Europe by farmers, public and private agencies and policy makers to a greater extent for decision making (Murthy, 2012). In addition, basic knowledges about inputs provide valuable informations applicable in yield prediction. There are also many studies showing the benefits of crop prediction and geostatistical analysis for agricultural management (Seelan et al., 2003).

It is clear that many inputs data play a key role in yield prediction and crop simulations. Nevertheless appropriate data collection can be limited for farmers in practical use. The main aim of this study is to use only the most common data from agronomical praxis as yield, mostly free satellite images and weather data (temperature and precipitation) and phenology expressed by BBCH scale for yield or NDVI frequency maps modelling for the yield prediction and crop structure estimation.

MATERIALS AND METHODS

Study area

The study area is an 24.7 ha experimental field located near to Vendolí village (N 49°43'48", E 16°24'14"), The Czech Republic. The experimental field is undulated with elevation ranges from 543 m to 571 m a.s.l. and 6% slope. The soil can be classified as modal cambisols on limestone sandstones. Some parts of this plot are strongly eroded, especially those sloping. The average precipitation is 700 mm per year and the average temperatures ranges between 6 and 7 °C. Table 1 contents the temperature and precipitation data from monitored years (2014 to 2018). The experimental field is owned by Agricultural Company Vendolí used conventional arable soil technology (ploughing) on all their plots. Since 2014 the crop rotation has been as follows: winter wheat (2014), spring barley (2015), winter rape (2016), winter wheat (2017) and spring barley (2018).

Table 1. Weather conditions (precipitations and temperatures) at different phenological phases by BBCH scale for experimental field in 2014–2018

	Precipitation (mm)					Temperature (°C)				
	2014	2015	2016	2017	2018	2014	2015	2016	2017	2018
BBCH 0–19	37.0	30.4	69.0	32.8	21.1	8.8	5.5	12.1	3.6	15.2
BBCH 20–29	97.8	7.6	191.0	224.2	37.7	2.8	9.7	3.0	2.7	17.0
BBCH 30–59	127.2	35.8	44.2	75.9	24.8	9.6	13.0	6.7	16.1	19.8
After BBCH 60	201.8	132.6	177.5	173.8	53.8	17.1	18.6	15.9	19.6	19.4
Sum	463.8	206.4	481.7	506.7	137.4	-	-	-	-	
Mean	115.9	51.6	120.4	126.7	34.4	9.6	11.7	9.4	10.5	17.9

Yield and remote sensing data

The yield was measured by a combine harvester New Holland CR9080 equipped with yield monitor and DGPS receiver with EGNOS correction. The accuracy of this system is ± 0.1-0.3 m in horizontal and ± 0.2–0.6 m in vertical direction. The yield data are saved every 1 second with coordinates to the external memory. Failure on external memory caused the data loses in 2017. The yield data were process by basic statistical method in order to eliminate the errors of yield measurement system. The yield data sets were then interpolated to kriging maps (see Fig. 1) using experimental variograms. Details about yield data processing are more described in Kumhálová et al., 2011. Relative yield values were calculated for each yield data set with the aim to standardize the yield data (the actual yield value to average yield value of the plot converted to percentages). The relative yield maps were then converted to rasters, resampled to equal spatial resolution (10 m according to Sentinel 2 spatial resolution) and recalculated to yield frequency maps (Maphanyane et al., 2018) with help of Cell Statistics tool in ArcGIS 10.4.1 SW (ESRI, Redlands, CA, USA). The maximum values of the input's yield data were used for yield frequency maps calculation. The yield frequency maps were derived from the all measured years and from cereals only (except winter rape yield) – see Fig. 2, (a, b).

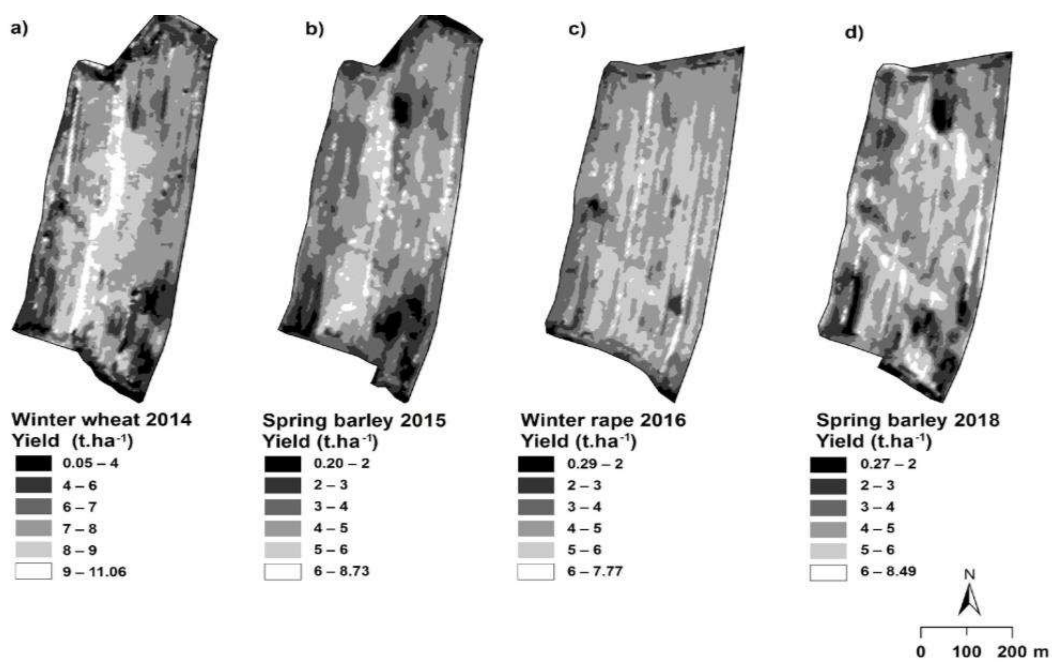

Figure 1. Yield maps (in t ha^{-1}) for the years 2014 with winter wheat (a); 2015 with spring barley (b); 2016 with winter rape (c); 2018 with spring barley (d).

The Landsat 8 satellite image for 2014 was downloaded from USGS (https://earthexplorer.usgs.gov/), Sentinel 2A images for 2016, 2017 and 2018 were downloaded from Copernicus Open Access Hub (https://scihub.copernicus.eu/) and SPOT 7 image for 2015 was purchased from ArcDATA Company (https://www.arcdata.cz/). The last satellite images from each vegetation season were selected, pre-processed to the level of BOA reflectance (Bottom of Atmosphere) and resampled to 10 m spatial resolution except Landsat image in 2014 (see Table 2 and

Fig. 3) with the help of SW ENVI 5.5 (Excelis, Inv. Mc Lean, USA) or SNAP 6.0.4 (ESA, http://step.esa.int/main/). Normalized Difference Vegetation Index was calculated from each image. NDVI frequency maps with the help of Cell Statistics tool were created in four variations, where maximum values of the input data were used. The NDVI frequency maps were derived on the base of – all NDVI images [1], NDVI images for cereals only (without 2016 – winter rape) [2], all NDVI images except 2014 (with 30 m spatial resolution/Landsat image) [3] and NDVI for cereals (except 2014 and 2016) [4] – see Fig. 2(c–f).

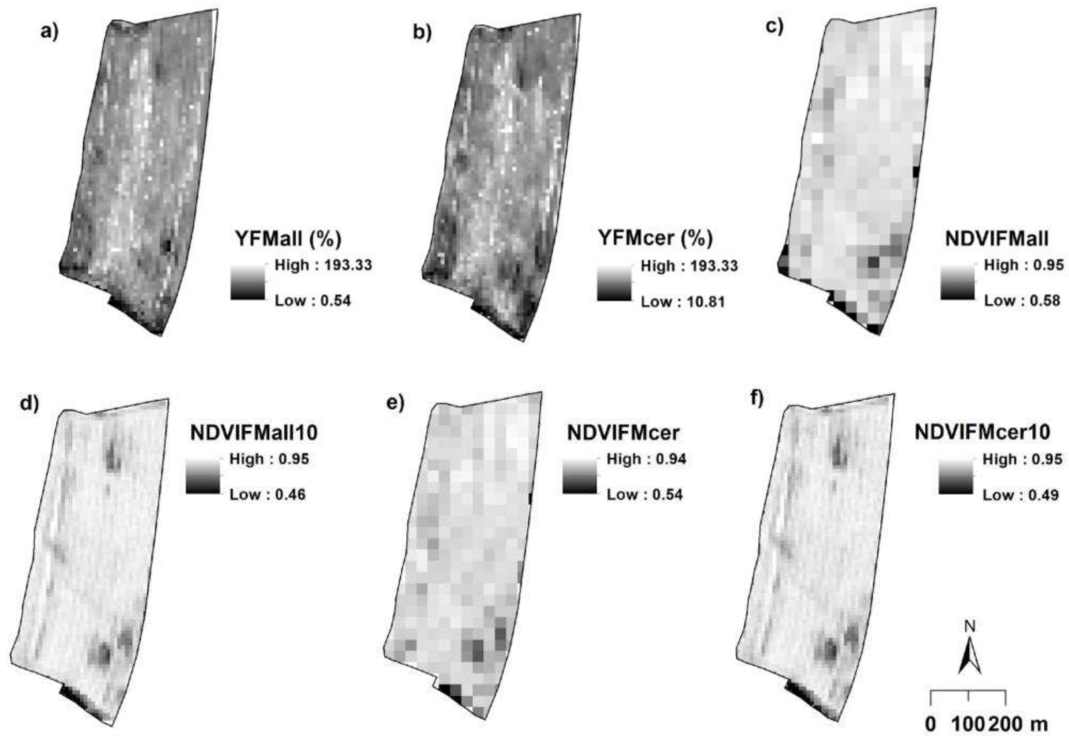

Figure 2. Yield and Normalised Difference Vegetation Index (NDVI) frequency maps: YFMall = yield frequency map derived from all yield maps (a); YFMcer = yield frequency map derived from cereals yield maps only (b); NDVIFMall = NDVI frequency map for all years (c); NDVIFMall10 = NDVI frequency map for all years without Landsat image/2014 (d); NDVIFMcer = NDVI frequency map derived for cereals only (e); NDVIFMcer10 = NDVI frequency map derived for cereals without Landsat image/2014 (f).

Table 2. Satellite images used in this study

Satellite	Sensor	Spatial resolution	RED range (nm)	NIR range (nm)	Date
Landsat 8	OLI	30 m	636–673	851–879	7-July 2014
SPOT 7	NAOMI	6 m	625–695	760–890	4-July 2015
Sentinel 2A	MSI	10 m*	650–680	785–900	5-June 2016
					20-June 2017
					17-June 2018

RED = reflectance in RED band; NIR = reflectance in near infrared band; OLI = Operational Land Imager; NAOMI = New AstroSat Optical Modular Instrument; MSI = Multispectral Instrument; * 10 m for RED and NIR bands.

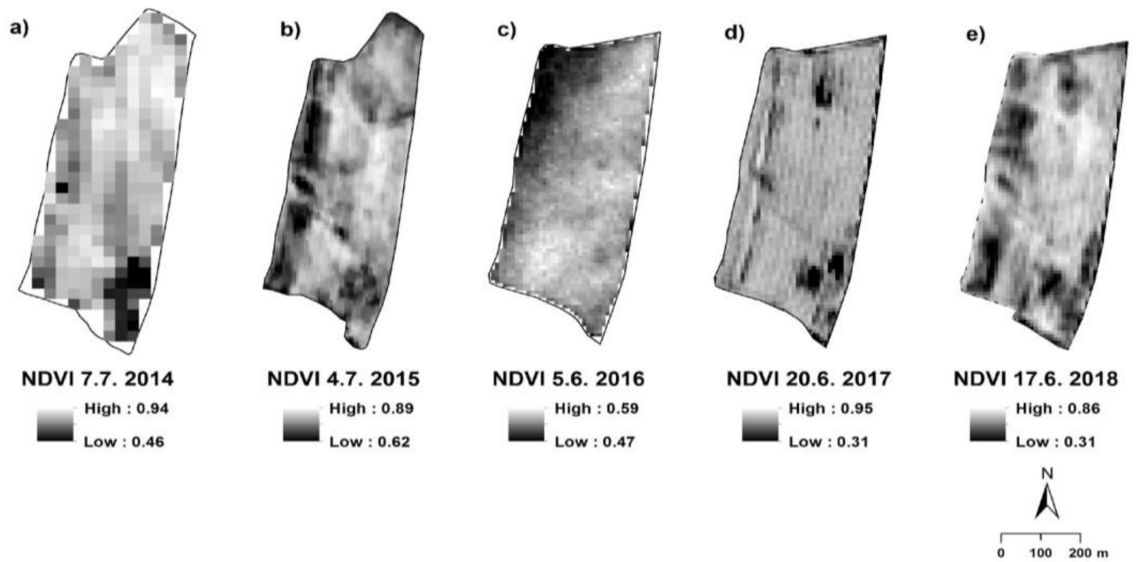

Figure 3. Normalised difference Vegetation Index (NDVI) for the years 2014 with winter wheat (a); 2015 with spring barley (b); 2016 with winter rape (c); 2017 with winter wheat (e); 2018 with spring barley (f).

Coefficients of determination were calculated in Statistica 8.0 SW (StatSoft Inc., Tulsa, OK, USA) between each crop yield data, NDVI images, yield frequency maps and NDVI frequency maps (see Table 3 and 4).

RESULTS AND DISCUSSION

The coefficients of determination for selected parameters are shown in Table 3 and 4. The coefficients of determination were calculated for a 5% significance level.

Table 3. Coefficients of determination between yield from selected years and Yield/NDVI frequency maps and NDVI (at 5% significance level)

Models	Yield 18	Yield 16	Yield 15	Yield 14
YFMcer	0.56	0.15	0.59	0.45
YFMall	0.24	0.16	0.46	0.44
NDVIFMcer	0.12	0.01	0.22	0.14
NDVIFMcer10	0.24	0.03	0.24	0.13
NDVIFMall	0.10	0.31	0.07	0.07
NDVIFMall10	0.30	0.08	0.36	0.16
NDVI180617	0.52	0.10	0.36	0.16
NDVI170620	0.27	0.08	0.34	0.16
NDVI160605	0.05	0.13	0.05	0.03
NDVI150704	0.18	0.09	0.27	0.08
NDVI140707	0.06	0.05	0.26	0.19

NDVI = Normalised Difference Vegetation Index for selected terms; YFMcer = yield frequency map derived from cereals yield maps only; YFMall = yield frequency map derived from all yield maps; NDVIFMcer = NDVI frequency map derived for cereals only; NDVIFMcer10 = NDVI frequency map derived for cereals without Landsat image/2014; NDVIFMall = NDVI frequency map for all years; NDVIFMall10 = NDVI frequency map for all years without Landsat image/2014.

Table 4. Coefficients of determination between NDVI from selected terms and Yield/NDVI frequency maps (at 5% significance level)

	NDVI180617	NDVI170620	NDVI160605	NDVI150704	NDVI140707
YFMcer	0.38	0.24	0.04	0.17	0.14
YFMall	0.18	0.16	0.08	0.12	0.14
NDVIFMcer	0.20	0.31	0.006	0.12	0.35
NDVIFMcer10	0.18	0.38	0.008	0.07	0.14
NDVIFMall	0.06	0.03	0.14	0.06	0.05
NDVIFMall10	0.26	0.96	0.02	0.12	0.18

NDVI = Normalised Difference Vegetation Index for selected terms; YFMcer = yield frequency map derived from cereals yield maps only; YFMall = yield frequency map derived from all yield maps; NDVIFMcer = NDVI frequency map derived for cereals only; NDVIFMcer10 = NDVI frequency map derived for cereals without Landsat image/2014; NDVIFMall = NDVI frequency map for all years; NDVIFMall10 = NDVI frequency map for all years without Landsat image/2014.

Table 3 showed that winter rape yield prediction based on yield frequency maps had lower usability ($r^2 = 0.15$ /0.16 for both cases) than the yield prediction maps for cereals yield estimations (r^2 from 0.24 to 0.59). On the other hand the cereals yield prediction was more accurate for model which included the yield form cereals only (except winter rape, see Fig. 2, b). The yield frequency map for cereals explained from 56% to 59% of actual yield variability for spring barley and 45% for winter wheat yield. No significant difference was found in yield prediction for winter wheat in 2014 between both yield models (see Fig. 2, a and b). On the contrary yield frequency map for cereals (see Fig. 2b) explained actual spring barley yield more significantly than the other model.

NDVI frequency map from all year except 2014 with Landsat image, resampled to 10 m (see Fig. 2, d), seemed to be the best model for actual cereal yields explaining. Nevertheless the actual yields were explained from 30 to 36% for spring barley and 16% for winter wheat. Winter rape actual yield was best explained, but not too much significantly (31%), by the model derived from all NDVI from 2014 to 2018 (see Fig. 2, c).

Coefficients of determination between actual yields and actual NDVI map generally fits best for individual years. The exception was NDVI in 2018, where NDVI image fits best for both spring barley yield maps (in 2015 and 2018 – see Figs 1 and 3).

Table 4 showed coefficient of determination between NDVI from selected terms and Yield / NDVI models. The models generally better explain the cereal crop variability, crop health and structure in individual terms in years 2017 and 2018. It can be caused by weather conditions, when ore water supply was during crop tillering (BBCH 20–29) with higher temperature in comparison with previous years. The best model for crop condition estimation seems to be the NDVI frequency map in spatial resolution of 10 m according to Sentinel 2 image from all years except 2014 (see Fig. 2, d). This model explains winter wheat crop structure from 96%. The best model for crop yield estimation is then yield frequency map for cereals (see Fig. 2, b) that explain the yield variability from 44% in average for all selected years.

The yield is made up of many variables among which belong especially weather condition, soil type, pH, soil nutrients and topography (Kumhálová et al. 2011). In time of climate warming it is obvious that the crop growth and then resulting yield is mostly influenced by water supply as in our study in 2017 and 2018. Crops benefit better in places with better water and nutrients supply, especially in drier years. This statement is in accordance with Schmidt & Persson (2003) or Kumhálová & Matějková (2017). The places with better productivity are good bounded by derived yield or NDVI frequency maps. Each of these models used in this study has its positive or negative sides that can influence their usability. The yield frequency maps depend on annual measurement of yield data. It can be a problem for farmers who do not have the appropriate equipment (active yield monitor on combine harvester). The problem may also occur during recording and storing yield data on combine harvester. This was case of our study in 2017. In order to obtain as accurate data as possible, it is necessary to calibrate the yield monitor system and to properly process the yield data using advanced tools (Chung et al., 2002, Maldaner et al., 2016). Currently, many commercial or freely available softwares allow relatively simple data processing to resulting yield frequency map (Pink & Dobermann, 2005). The NDVI frequency maps depend on satellite images access. Currently satellite images from Copernicus Earth observation programme offers optical satellite images with high spatial (from 10 to 60 m) and radiometric (13 bands) resolution and very good revisit frequency (5-days on equator). Fiuzal et al. (2017) stated that the main limitation of using optical data is heavy cloud cover. This is in accordance with our study. The satellite images were selected according to criteria (1) last satellite image in vegetation season and (2) cloud-free image. For this reason, there is a relatively large data range in the images used for the purposes of this study (5 June 2016 and 7 July 2014). To ensure these criteria, it was also necessary to use various satellite images (Landsat, Sentinel 2 and SPOT) regardless of their properties. The spectral and spatial differences can be one of the limitations in comparison and use data sets. This corresponds well with Scudiero et al. (2016) study, where the suitability of sensor measurements to geographical region and use purposes was assessed.

Many studies have been written to evaluate cereals using optical remote sensing. The first was publicated in the 1970s with the most widely used NDVI spectral index. As can be seen from the results of this study, the models used are more suitable to evaluate and predict the yield of cereals than winter rape. Our results are in good agreement with the findings of Domínguez et al. (2017). They found out that different winter rape canopy architecture and leaf structure cause different spectral properties then in the case of cereals. Winter rape crops have also other growth requirements than cereals.

CONCLUSIONS

The results showed that information about crop yield and crop condition derived from satellite images can be useful for frequency map modelling. Yield frequency map and NDVI frequency map can be helpful tool for agriculture plots management. These models have their limitations that can be crucial for agricultural praxis. Nevertheless, our study showed that the best model for crop yield estimation is yield frequency map for cereals explaining the yield variability from 44% in average for all selected years. The best model for crop condition estimation seems to be the NDVI frequency map in spatial resolution of 10 m according to Sentinel 2 image from all years. This model explain winter wheat crop structure from 96% and from 38% for all selected NDVI images. The models were more significant for cereals and in drier and warmer years.

ACKNOWLEDGEMENTS. This study was supported by Czech University of Life Sciences Prague, when conducted under grant IGA no. 31180/1312/3118. The authors wish to deep thank the farmers in Agricultural Company Vendolí for their time, inputs data and provided experimental field.

REFERENCES

Asrar, G., Fuchs, M., Kanemasu, E.T. & Hatfield, J.L. 1984. Estimating absorbed photosynthetic radiation and leaf-area index from spectral reflectance in wheat. *Agron. J.* **76**, 300–306.

Baret, F. & Guyot, G. 1991. Potentials and limits of vegetation indexes for LAI and APAR assessment. *Remote Sens. Environ*. **35**, 161–173.

Copernicus Open Access Hub. *https://scihub.copernicus.eu/* Accessed 18.12.2018.

Chung, S.O., Sudduth, K.A. & Drummond, S.T. 2002. Determining yield monitoring system delay time with geostatistical and data segmentation approaches. *Transactions of the ASAE* **45**(4), 915–926.

Domínguez, J.A., Kumhálová, & J. Novák, P. 2017. Assessment of the relationship between spectral indices from satellite remote sensing and winter oilseed rape yield. *Agronomy Research* **15**, 055–068.

Fieuzal, R., Marais Sicre, C. & Baup, F. 2017. Estimation of corn yield using multi-temporal optical and radar satellite data and artificial neural networks. *International Journal of Applied Earth Observation and Geoinformatio*n **57**, 14–23.

Gianquinto, G., Orsini, F., Fecondini, M., Mezzetti, M., Sambo, P. & Bona, S. 2011. A methodological approach for defining spectral indices for assessing tomato nitrogen status and yield. *Eur. J. Agron.* **35**(3), 135–143.

Knipling, E.B. 1970. Physical and physiological basis for the reflectance of visible and near-infrared radiation from vegetation. *Remote Sens. Environ*. **3**, 155–159

Kumhálová, J., Kumhála, F., Kroulík, M. & Matějková, Š. 2011. The impact of topography on soil properties and yield and the effects of weather conditions. *Precision Agriculture* **12**, 813–830.

Kumhálová, J. & Matějková, Š. 2017. Yield variability prediction by the remote sensing sensors with different spatial resolution. *International Agrophysics* **31**, 195–202.

Maldaner, L.F., Molin, J.P. & Canata, T.F. 2016. Processing yield data from two or more combines. In: *Proceedings of the 13th International Conference on Precision Agriculture (unpaginated, online).* Monticello, IL: International Society of Precision Agriculture. Accessed: *https://www.researchgate.net/publication/308168387* 19.10.2018.

Maphanyane, J.G., Mapeo, R.B.M. & Akinola, M.O. 2018. *Handbook of research on Geospatial Science and Technologies.* IGI Global, Hershey PA USA, 457 pp.

Moran, M.S., Clarke, T.R., Inoue, Y. & Vidal, A. 1994. Estimating crop water deficit using the relation between surface-air temperature and spectral vegetation index. *Remote Sens. Environ.* **49**, 246–263.

Mulla, D.J. 2013. Twenty five years of remote sensing in precision agriculture: Key advances and remaining knowledge gaps. *Biosystems Engineering* **114**(4), 358–371.

Murthy, V.R.K. 2002. Basic principles of Agricultural Meteorology. Book syndicate publishers, Koti, Hyderabad, India, 261 pp.

Pink, J.L. & Dobermann, A. 2005. Processing of Yield Map Data. *Precision Agriculture* **6**, 193–212.

Rosenzweig, C., Jones J.W, Hatfield J.L., Ruane, A.C., Boote, K.J., Thorburn, P., Antle, J.M., Nelson, G.C, Porter, C., Janssen, S., Asseng, S., Basso, B., Ewert, F., Wallach, D., Baigorria, G. & Winter, J.M. 2013. The Agricultural Model Intercomparison and Improvement Project (AgMIP): Protocols and pilot studies. *Agric. Forest Meteorol*. **170**, 166–182.

Rouse, J.W., Haas, R.H., Schell, J.A. & Deering, D.W. 1974. Monitoring vegetation systems in the Great Plains with ERTS. In: *Freden, S. C., Mercanti, E. P., Becker, M. (Eds.), Third Earth Resources Technology Satellite-1 Symposium,* Vol. 1: Technical Presentations, NASA SP-351. National Aeronautics and Space Administration, Washington, DC, pp. 309–317.

Schmidt, F. & Persson, A. 2003. Comparison of DEM data capture and topographic wetness indices. *Precision Agriculture* **4**, 179–192.

Scudiero, E., Corwin, D.L., Wienhold, B.J., Bosley, B., Shanahan, J.F. & Johnson, C.K. 2016. Downscaling Landsat 7 canopy reflectance employing a multi-soil sensor platform. *Precision Agriculture* **17**, 53–73.

Seelan, S.K., Languette, S., Casady, G.M., Seielstad, G.A. 2003. Remote sensing applications for precision agriculture: A learning community approach. *Remote Sensing of Environment* **88**, 157–169.

SNAP 6.0.4. ESA. *http://step.esa.int/main/* Accessed 19.12.2018.

Thornton, P.K., Bowen, W.T., Ravelo, A.C., Wilkens, P.W., Farmer, G., Brock, J. & Brink, J.E. 1997. Estimating millet production for famine early warning: an application of crop simulation modelling using satellite and ground-based data in Burkina Faso. *Agricultural and Forest Meteorology* **83**, 95–112.

Tucker, C.J., Holben, B.N., Elgin, J.H. & McMurtrey III, J.E. 1981. Remote sensing of total dry matter accumulation in winter wheat. *Remote Sens. Environ*. **11**, 171–189.

USGS. *https://earthexplorer.usgs.gov/* Accessed 19.12.2018.

Wardlow, B.D. & Egbert, S.L., 2008. Large-area crop mapping using time-series MODIS 250 m NDVI data: an assessment for the U.S. Central Great plains. *Remote Sens. Environ*. **112**, 1096–1116.

Xue, J. & Su, B. 2017. Significant remote sensing vegetation indices: a review of developments and applications. *Journal of Sensor*, 2017, 17.